Exploring Underlying Correlations in Multi-Fidelity Finite Element Simulations of Open-Hole Tension Tests: A Comparative Study Using Machine Learning

Amirali Eskandariyun; Huilong Fu; Johannes Reiner; Reza Vaziri; Navid Zobeiry

OFFICIAL CONFERENCE PUBLICATION

Proceedings of the American Society for Composites - Thirty-Eighth Technical Conference (2023)

https://doi.org/10.12783/asc38/36670

RELATED SUBSTANTIALLY EXTENDED JOURNAL ARTICLE

A. Eskandariyun, H. Fu, and N. Zobeiry, "An Integrated Process-Failure Simulation Framework for Predicting Composite Allowables via Multi-Fidelity Stochastic Simulation and Machine Learning," Composites Part B 326, 114051 (2026).

https://doi.org/10.1016/j.compositesb.2026.114051

ABSTRACT

Certification of composite aerostructures is typically achieved via analysis supported by testing, following the building block approach. Analysis of failure and crash at different scales, as well as design iterations and optimization, require fast and validated numerical models. Given the complexity and interactions of multi-failure mechanisms in composites, high-fidelity FE models are often needed to explicitly simulate the behavior of individual layers and their interlaminar interfaces, using a mix of continuum and discrete damage models. However, high-fidelity FE models require a considerable amount of time to set up, calibrate, and perform. On the other hand, low-fidelity modeling approaches, such as laminate-based smeared models, may provide reduced accuracy in some cases, while offering shorter simulation times and thereby lower computational costs.

In this study, progressive failure of Open-Hole Tension (OHT) tests on HEXCEL IM-7/8552 quasi-isotropic laminates are investigated using both low- and high-fidelity FE models. A Machine Learning (ML) technique is then employed to perform a comparative study between the inputs and outputs of these models. The ultimate goal is to identify areas in the FE parameter space where the low-fidelity model can be used as a substitute for the high-fidelity model with reasonable accuracy and to discover the relationships among main parameters to reproduce high-fidelity results from the low-fidelity model in an accelerated manner. To generate the low-fidelity model, a laminate-based FE model was created in LS-DYNA, using a continuum elasto-plastic damage-based material card, MAT081. The model parameters were varied randomly, and simulations were performed to generate a large database of low-fidelity FE results. Similarly, a ply-based FE model employing MAT261 for continuum intralaminar damage modeling combined with cohesive tiebreak contacts to capture discrete interlaminar delamination was created. This high-fidelity model was also used to generate another database of simulation results. Both databases were used to create a training set for an ML model, aiming to study the correlation between low- and high-fidelity inputs that result in similar failure responses. The results enable increasing use of low-fidelity FE models to generate data for the training of ML models.

Amirali Eskandariyun[1], Huilong Fu[1], Johannes Reiner[2], Reza Vaziri[3], Navid Zobeiry[1]*

1 University of Washington, Seattle, WA 98195, United States

2 Deakin University, Geelong, VIC 3220, Australia

3 University of British Columbia, Vancouver, BC V6T 1Z4, Canada

INTRODUCTION

Advanced composite materials are increasingly being utilized in aerospace components due to their exceptional specific strength and stiffness. Additionally, composites exhibit higher resistance against fatigue and corrosion, compared to their metallic counterparts, enabling the development of efficient designs while ensuring the safety of aerospace structures. In recent years, prominent aircraft models such as the Boeing 787 and Airbus A350 are composed of composites constituting at least 50% of their total weight [1]. It is anticipated that the utilization of composites in aerospace structures will continue to experience substantial growth in future designs.

Analytical tools are essential for the design, manufacturing, and certification processes of composites. They enable engineers to predict and analyze performance, optimize designs, identify manufacturing issues, and provide analysis supported by tests for certification purposes [2]. One of the most well-established tools for failure analysis of composites is the finite element (FE) method [3]. Failure analysis by FE can be conducted using both low-fidelity and high-fidelity configurations. While low-fidelity approaches may yield lower accuracy, they offer the advantage of faster and more cost-effective analysis. On the other hand, high-fidelity approaches are computationally more demanding, despite their relatively higher accuracy [4], [5].

Although high-fidelity models strive to incorporate as many underlying physics and geometry aspects of the problem as possible, low-fidelity and reduced-order modeling techniques are employed by intentionally neglecting one or more components from the model while minimizing the loss in overall accuracy. Low-fidelity finite element (FE) approaches are achieved through various techniques, including reducing dimensions (from 3D to 2D or 1D), implementing coarser meshing, simplifying elemental calculations, and assuming continuum elements for discrete structures [6]. In reduced-order modeling approaches, the principal mechanisms contributing to the outcome are included, while secondary mechanisms are often neglected in the analysis.

For failure analysis of composites, a low-fidelity analysis approach involves representing the entire laminate or sub-laminate as a continuum and disregarding the individual ply-level and interlaminar interactions. While this method has its own limitations and drawbacks including the inability to explicitly consider delamination, it provides fast and relatively reliable responses in some configurations including dispersed quasi-isotropic lay-ups [7]. It is worth mentioning that fast simulation is required for model calibration, allowables prediction at the coupon-level, and design optimization at larger scales [8]. Finding the specific ranges of FE parameters in which the low-fidelity model can perform as well as the high-fidelity model is always challenging.

Given the notch sensitivity of composites, the open-hole tension (OHT) test is one of the key tests in the building block approach for generating allowables at the coupon-level [9]. Validating numerical models for this crucial coupon is one of the basic requirements of the design and certification of composite aircraft [10]. In this study, we performed both low- and high-fidelity FE simulations on open-hole tension test coupons using the smeared damage approach at the laminate level to implicitly include the effect of discrete failure mechanisms such as splitting and delamination, and a ply-based approach to explicitly include the effect of delamination. Using both methods, a large number of simulations were performed by randomly varying FE inputs. The datasets from these simulations were analyzed using machine learning techniques to compare the accuracy of models and to find the areas of FE inputs in which we can rely on a low-fidelity model and areas in which we need correction factors to produce acceptable results from it. The results provide an effective guideline for accurately applying low-fidelity modeling for notch sensitivity analysis in composites.

MATERIALS AND METHODS

In this study, we are performing explicit FE analysis, using the LS-DYNA package on OHT coupon. For the material system, we have used HEXCEL IM7/8552 which is a well-studied carbon fiber reinforced composite (CFRP) [11], [12]. The coupon layup consists of 16 layers of quasi-isotropic laminate with $[45/0/-45/90]_{2s}$ layup. The geometry, loading, and boundary conditions are presented schematically in Figure 1 below [13].

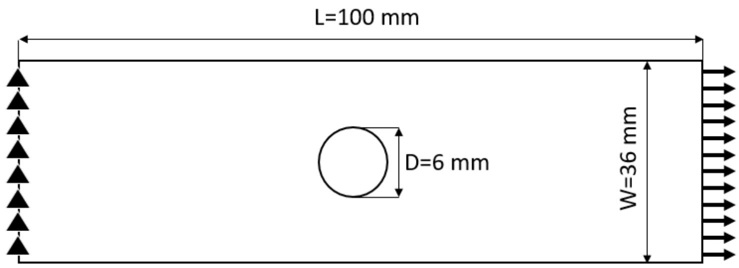

Figure 1. Schematic preview of the model's geometry and boundary conditions

Finite Element Models

In the current investigation, we employed the LS-DYNA explicit finite element (FE) package to conduct simulations encompassing both low-fidelity and high-fidelity approaches. In the scope of this study, we utilized the MAT081 material model for low-fidelity modeling [14]. MAT081 is an isotropic elasto-plastic damage material model that has been successfully used for simulating composite failure by accounting for the complex failure of the laminate using the calibrated strain-softening response of an element [15]–[17]. In this laminate-based approach, since the interlaminar behavior of composites is not simulated, the computational cost as well as the calibration effort is significantly reduced. For a simple linear strain-softening damage response, only three parameters are needed for model calibration: Young's modulus (related to the stiffness of the element), fracture energy (related to the damage saturation strain of the element), and continuum laminate-based strength (related to damage initiation strain of the element). It should be noted that it is a common practice to scale the damage saturation strain in such approaches based on the element size and following Bazant's crack band scaling law. A schematic representation of the laminate-based model is available in Figure 2.

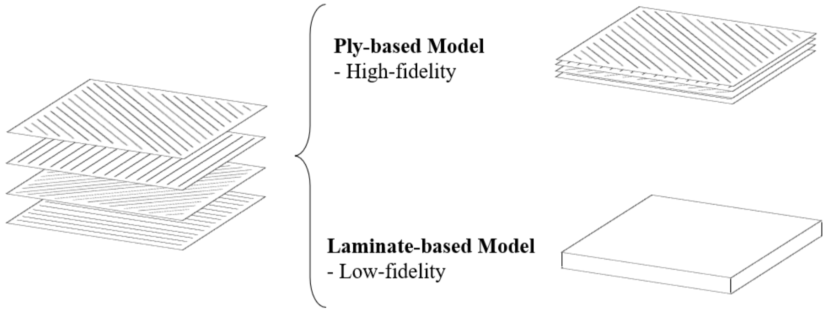

Figure 2. Graphical illustration of approaches used in this study for high- and low-fidelity models.

For the high-fidelity model, in the present study, we incorporated LS-DYNA's MAT261, which is an orthotropic damage-based material model specifically developed for composites failure by Pinho et al [18]. This model has been used in several applications for failure prediction of CFRP composites [13], [19]. It uses physical-based failure criteria to provide a representation of the ply-by-ply failure behavior [20]. For the interlaminar modeling, we used cohesive tie-break contact in LS-DYNA to represent the delamination by utilizing the mode I/II tractions and energies [21]. Although more physics is included in this model, the complexity in modeling, as well as the several additional parameters needed for the failure model, makes it much less cost-effective in comparison to the laminate-based model mentioned earlier. Please refer to Figure 3 for better illustrations of the two models.

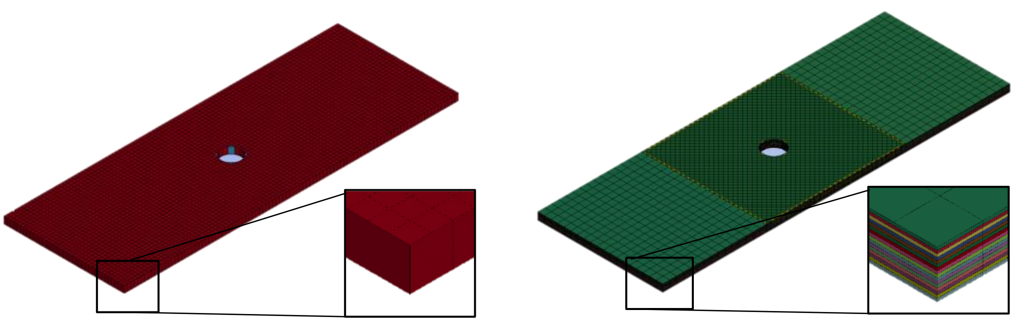

Figure 3. Low-fidelity (left) and high-fidelity (right) models as visualized in LS-PrePost®

For the low-fidelity model, aside from isotropic elastic properties, elemental strength, and fracture energy (S_e and G_f) are used as variables. For the high-fidelity model, there are 14 strength and energy parameters to be calibrated (10 for intralaminar and 4 for interlaminar failure properties). To reduce the number of parameters and focus only on the main contributing parameters, an initial sensitivity analysis was performed by generating 400 realizations of the high-fidelity model while varying all the parameters within their respective reasonable ranges. We could then analyze the sensitivity of each parameter on the final strength of the OHT coupon. Among the 14 parameters, we narrowed down to two governing parameters in this coupon, which were

doi.org/10.12783/asc38/36670

intralaminar strength (X_t), and mode II interlaminar (delamination) fracture energy (G_{II}). Some examples of the sensitivity analysis results are available in Figure 4 below.

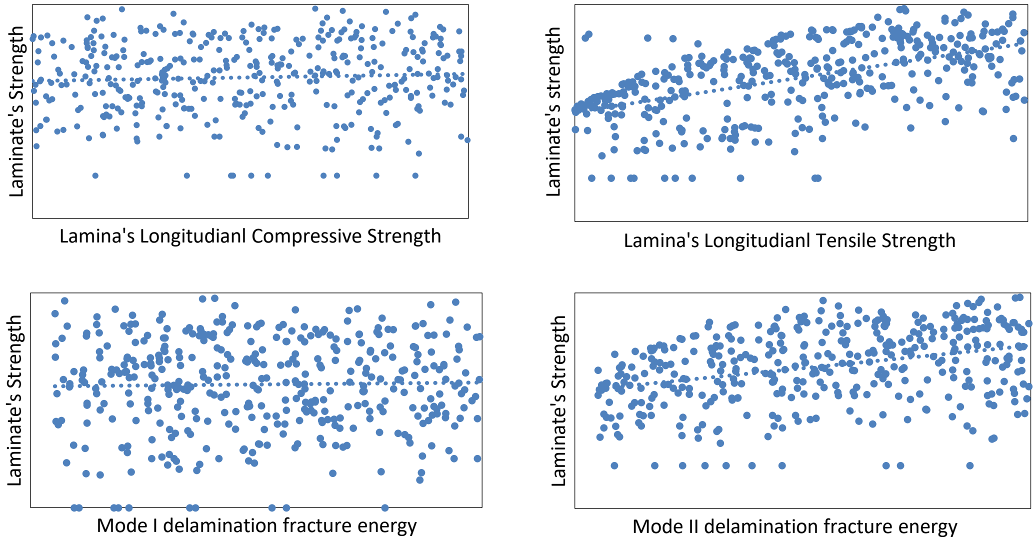

Figure 4. Examples of the sensitivity analysis for high-fidelity model's parameters

Based on the performed sensitivity analysis in the previous step and the data available in the literature for elastic and strength properties of IM7/8552 lamina, we could specify the fixed parameters and ranges of variables for both models to simulate the OHT coupon failure [22]–[26]. It should be noted that the elastic properties of the quasi-isotropic laminate to be used in the low-fidelity model were calculated using IM7/8552 lamina properties and based on the classical lamination theory (CLT) [27]. Values used for the fixed and variable parameters for both models are available below in Tables I and II. The parameters are categorized and reported as elastic and failure properties, respectively.

TABLE I. IM7/8552 ELASTIC PROPERTIES USED IN THE HIGH-/LOW-FIDELITY SIMULATION OF THE OHT COUPON [22]–[25]

High-fidelity Elastic Parameters	**Values/ Ranges**	**Low-fidelity Elastic Parameters**	**Values/R anges**
Longitudinal Modulus E_{11}	161 GPa	Calculated Elemental Young's Modulus (E_e)	61.7 GPa
Transverse Modulus $E_{22}=E_{33}$	11.4 GPa	Calculated Elemental Shear Modulus (G_e)	23.2 GPa
In-plane Shear Modulus G_{12}	5.17 GPa	Calculated Elemental Poisson's Ratio (υ_e)	0.332
Out-of-plane Shear Modulus G_{23}	3.98 GPa		
In-plane Poisson's ratio υ_{21}	0.023		
Out-of-plane Poisson's ratio υ_{32}	0.436		

doi.org/10.12783/asc38/36670

TABLE II. FIXED AND VARIABLE RANGES FOR DAMAGE PROPERTIES OF IM7/8552 USED IN THE HIGH-/LOW-FIDELITY SIMULATION OF THE OHT COUPON [22]–[26]

High-fidelity Damage Parameters	Values/ Ranges	Low-fidelity Damage Parameters	Values/ Ranges
Longitudinal Tensile Strength X_T	**0.7 - 3.8 GPa**	Elemental Tensile Strength S_e	**0.4 - 1.9 GPa**
Longitudinal Compressive Strength X_C	1.20 GPa	Elemental Fracture Energy G_f	**50 - 150 kJ/m^2**
Transverse Tensile Strength Y_T	111 MPa		
Transverse Compressive Strength Y_C	199.8 MPa		
In-plane Shear Strength S_L	92.3 MPa		
Fiber Tensile Fracture Energy G_f^T	196.2 kJ/m^2		
Fiber Compressive Fracture Energy G_f^C	80 kJ/m^2		
Matrix Longitudinal Fracture Energy G_m^L	0.38 kJ/m^2		
Matrix Transverse Fracture Energy G_m^T	0.26 kJ/m^2		
Shear Fracture Energy G_{IIC}	1.34 kJ/m^2		
Interlaminar Failure Stress (Normal) S_n	60 MPa		
Interlaminar Failure Stress (Shear) S_s	90 MPa		
Interlaminar Mode I Fracture Energy G_I	0.2 kJ/m^2		
Interlaminar Mode II Fracture Energy G_{II}	**0.2 - 1.8 kJ/m^2**		

Consequently, we performed 50 high-accuracy high-fidelity simulations, each taking about 2 hours, based on randomly generating the aforementioned governing parameters. On the other hand, based on the very short amount of time required to simulate the low-fidelity model, 1200 simulations were performed, each taking 2.5 minutes. The results of these simulations were collected and then transferred into the machine learning framework for further analysis.

Machine Learning Framework

Despite producing a relatively large amount of data points from low-fidelity simulations, only 50 data points were generated using the high-fidelity approach. This small amount of data may pose a challenge for machine learning analysis using traditional deep learning methods. However, probabilistic machine learning methods such as Gaussian process regression (GPR) have emerged as a promising regression method in such cases. By utilizing Bayesian inference and assuming a Gaussian distribution, this approach effectively handles limited data by considering uncertainty in predictions.

To analyze the data from FE models, we used GPR to examine both high-fidelity and low-fidelity models' outcomes. Firstly, we employed the GPR model to predict the strength of the Open-Hole Tension (OHT) specimen using given inputs for the high-fidelity model (X_t and G_{II}). Afterward, using the predicted OHT strength value, we employed another GPR model to inversely determine the input parameters of the low-fidelity model. This inverse prediction technique allowed us to establish a correlation between the input parameters of the low-fidelity and high-fidelity models to produce the same coupon-level behavior. Based on these, we can create a framework that leverages the predictions made by the fast low-fidelity model, but with the accuracy of high-fidelity modeling. Figure 5 shows a flowchart of the mentioned framework.

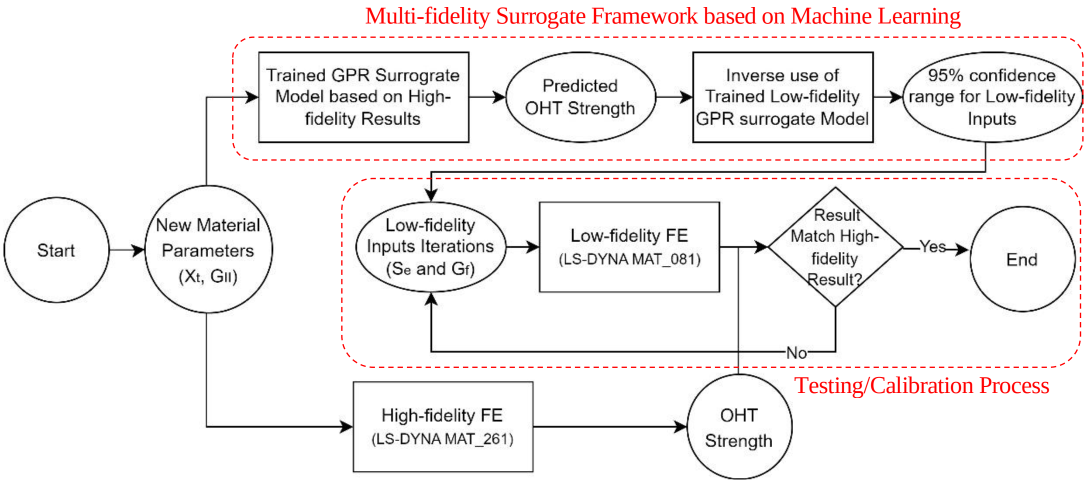

Figure 5. A flowchart illustrating the multi-fidelity framework, and the resulting calibrated low-fidelity model in comparison to high-fidelity FE modeling.

RESULTS AND DISCUSSION

The input parameters for both models were picked from a uniform distribution in a relatively large range to capture all the variabilities and to be able to compare the two models, as the inputs were different in nature. After performing 50 simulations for the high-fidelity model and 1200 simulations for the low-fidelity model, and recording the strengths of the OHT coupon, we observed a similar trend in the distributions in results. Results for OHT strength values are plotted in Figure 6 below.

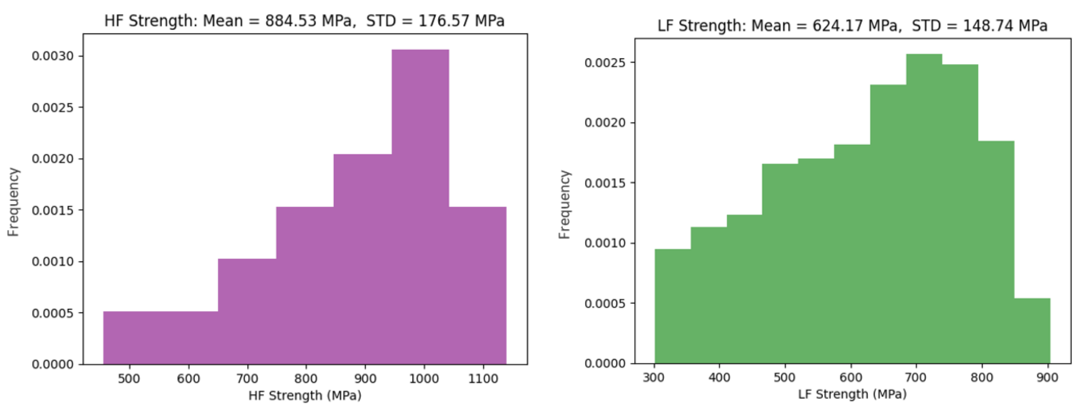

Figure 6. Distribution of resulted strength for high-fidelity (left) and low-fidelity (right) OHT models

Based on the results from both models, we performed GPR training using the input parameters and the OHT simulated strength values. Since the input values are not the same, we trained the GPR surface separately. A Matérn kernel was used as the GPR kernel and its parameters were trained to a score of about 99%. As mentioned in the previous section, one of the key advantages of GPR is that it can provide a probabilistic zone, which represents a 90% confidence interval. This confidence zone was used in predicting the corresponding low-fidelity input ranges for the calibration process (see Figure 5). Figure 7 illustrates the fitted GPR surfaces and the respective 90% confidence intervals (upper 95% and lower 5%), for both models.

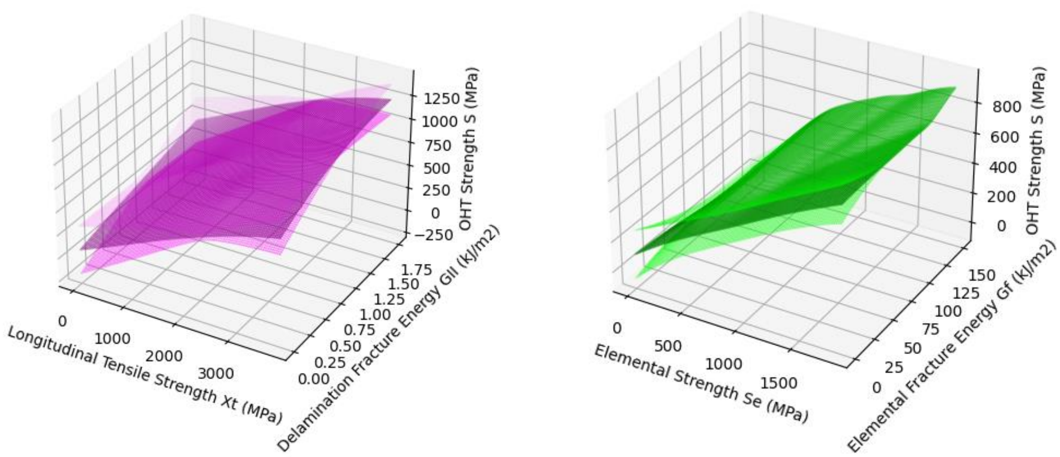

Figure 7. Trained GPR surface of the high-fidelity (left) and low-fidelity (right) showing OHT strength, based on initial respective parameters (light-colored surfaces show 95% confidence boundaries)

Testing and Validation

For testing the entire framework, we used 10% percent of the high-fidelity simulation results. Accordingly, the training set was chosen as 90% of the results. The input values of the testing set were introduced into the multi-fidelity surrogate framework. 90% confidence ranges for low-fidelity input parameters were extracted and used in the testing/calibration process (see Figure 5). The results of the testing process are available below in Table III.

TABLE III. MULTI-FIDELITY SURROGATE FRAMEWORK TESTING DATA

	HF parameters		**LF parameters**		**OHT Strength Discrepancy (%)**
	X_t (MPa)	**G_{II} (kJ/m^2)**	**S_e (MPa)**	**G_f (kJ/m^2)**	
1	2057	0.79	1586	83.1	4.8
2	720	0.40	883	59.8	0.9
3	971	1.52	1162	118.2	1.1
4	1371	1.00	1329	52.7	2.2
5	1489	1.68	1493	114.7	3.9

doi.org/10.12783/asc38/36670

CONCLUSIONS

The presented methodology shows substantial potential to correlate results from high-fidelity and low-fidelity models, specifically in the context of OHT failure analysis of quasi-isotropic laminates. While the accuracy of the combined ML and multi-fidelity modeling approach is comparable to that of high-fidelity simulation, the speed is similar to the speed of the low-fidelity modeling approach. The current framework has the flexibility to be extended to include more input parameters from both high and low-fidelity models and accommodate different coupon geometries. As shown in this study for OHT analysis, not all input parameters may be equally impactful for a given geometry. As such, it is important to conduct sensitivity analysis before training ML models. The accuracy and robustness of the framework can be further improved in the future, by training it with additional simulation data.

REFERENCES

[1] A. Hiken, “The Evolution of the Composite Fuselage - A Manufacturing Perspective,” *SAE International Journal of Aerospace*, vol. 10, no. 2, pp. 77–91, Sep. 2017, doi: 10.4271/2017-01-2154.

[2] P. Feraboli, “Composite Materials Strength Determination Within the Current Certification Methodology for Aircraft Structures,” 2009, doi: 10.2514/1.41286.

[3] R. Cumbo, A. Baroni, … A. R.-J. of C., and undefined 2022, “Design allowables of composite laminates: A review,” *journals.sagepub.com*, vol. 2022, no. 23, pp. 3617–3634, Sep. 2019, doi: 10.1177/00219983221117216.

[4] R. Vitali, R. T. Haftka, and B. V Sankar, “MULTIFIDELITY DESIGN OF STIFFENED COMPOSITE PANEL WITH A CRACK”.

[5] W. J. Vankan, B. A. T. Noordman, and K. Kueres, “High and low fidelity finite element modelling in aircraft composite fuselage structural analysis and optimisation,” 2013, Accessed: May 29, 2023. [Online]. Available: https://reports.nlr.nl/bitstream/10921/954/1/TP-2013-197.pdf

[6] V. L. Markine and V. V Toropov, “AIAA 2002-5651 USE OF HIGH-AND LOW-FIDELITY MODELS IN APPROXIMATIONS FOR DESIGN OPTIMIZATION,” 2002, doi: 10.2514/6.2002-5651.

[7] D. I. Gransden and R. Alderliesten, “Development of a finite element model for comparing metal and composite fuselage section drop testing,” *http://dx.doi.org/10.1080/13588265.2016.1273987*, vol. 22, no. 4, pp. 401–414, Jul. 2017, doi: 10.1080/13588265.2016.1273987.

[8] R. Cumbo, A. Baroni, … A. R.-J. of C., and undefined 2022, “Design allowables of composite laminates: A review,” *journals.sagepub.com*, vol. 2022, no. 23, pp. 3617–3634, Sep. 2019, doi: 10.1177/00219983221117216.

[9] E. Abisset, F. Daghia, and P. Ladevze, “On the validation of a damage mesomodel for laminated composites by means of open-hole tensile tests on quasi-isotropic laminates,” *Compos Part A Appl Sci Manuf*, vol. 42, no. 10, pp. 1515–1524, Oct. 2011, doi: 10.1016/J.COMPOSITESA.2011.07.004.

[10] S. H. Sanei, A. Arndt, and R. Doles, “Open hole tensile testing of 3D printed continuous carbon fiber reinforced composites”, doi: 10.1177/0021998320902510.

[11] P. P. Camanho, G. H. Erçin, G. Catalanotti, S. Mahdi, and P. Linde, “A finite fracture mechanics model for the prediction of the open-hole strength of composite laminates,” *Compos Part A Appl Sci Manuf*, vol. 43, no. 8, pp. 1219–1225, Aug. 2012, doi: 10.1016/J.COMPOSITESA.2012.03.004.

[12] M. W. Czabaj and J. G. Ratcliffe, “Comparison of intralaminar and interlaminar mode I fracture toughnesses of a unidirectional IM7/8552 carbon/epoxy composite,” *Compos Sci Technol*, vol. 89, pp. 15–23, Dec. 2013, doi: 10.1016/J.COMPSCITECH.2013.09.008.

[13] J. Reiner, X. Xu, N. Zobeiry, R. Vaziri, S. R. Hallett, and M. R. Wisnom, “Virtual characterization of nonlocal continuum damage model parameters using a high fidelity finite

element model," *Compos Struct*, vol. 256, Jan. 2021, doi: 10.1016/J.COMPSTRUCT.2020.113073.

[14] J. Reiner, "A practical approach for the non-local simulation of progressive damage in quasi-isotropic fibre-reinforced composite laminates," *Compos Struct*, vol. 265, p. 113761, Jun. 2021, doi: 10.1016/J.COMPSTRUCT.2021.113761.

[15] J. Reiner, R. Vaziri, and N. Zobeiry, "Machine learning assisted characterisation and simulation of compressive damage in composite laminates," *Compos Struct*, vol. 273, p. 114290, Oct. 2021, doi: 10.1016/J.COMPSTRUCT.2021.114290.

[16] N. Zobeiry, R. Vaziri, and A. Poursartip, "Characterization of strain-softening behavior and failure mechanisms of composites under tension and compression," *Compos Part A Appl Sci Manuf*, vol. 68, pp. 29–41, Jan. 2015, doi: 10.1016/J.COMPOSITESA.2014.09.009.

[17] J. Reiner, N. Zobeiry, and R. Vaziri, "A stacked sublaminate-based damage-plasticity model for simulating progressive damage in composite laminates under impact loading," *Thin-Walled Structures*, vol. 156, p. 107009, Nov. 2020, doi: 10.1016/J.TWS.2020.107009.

[18] S. T. Pinho, L. Iannucci, and P. Robinson, "Physically-based failure models and criteria for laminated fibre-reinforced composites with emphasis on fibre kinking: Part I: Development," *Compos Part A Appl Sci Manuf*, vol. 37, no. 1, pp. 63–73, Jan. 2006, doi: 10.1016/J.COMPOSITESA.2005.04.016.

[19] N. Zobeiry, J. Reiner, and R. Vaziri, "Theory-guided machine learning for damage characterization of composites," *Compos Struct*, vol. 246, p. 112407, Aug. 2020, doi: 10.1016/J.COMPSTRUCT.2020.112407.

[20] A. Rajaneesh, J. P. Ponthot, and M. Bruyneel, "High velocity impact response of composite laminates using modified meso-scale damage models," *Int J Impact Eng*, vol. 147, p. 103701, Jan. 2021, doi: 10.1016/J.IJIMPENG.2020.103701.

[21] F. Dogan, H. Hadavinia, … T. D.-C. E. J., and undefined 2012, "Delamination of impacted composite structures by cohesive zone interface elements and tiebreak contact," *Springer*, vol. 2, no. 4, pp. 612–626, 2012, doi: 10.2478/s13531-012-0018-0.

[22] S. Mukhopadhyay, M. I. Jones, and S. R. Hallett, "Tensile failure of laminates containing an embedded wrinkle; numerical and experimental study," *Compos Part A Appl Sci Manuf*, vol. 77, pp. 219–228, Oct. 2015, doi: 10.1016/J.COMPOSITESA.2015.07.007.

[23] M. May, S. Arnold-Keifer, and T. Haase, "Damage resistance of composite structures with unsymmetrical stacking sequence subjected to high velocity bird impact," *Composites Part C: Open Access*, vol. 1, p. 100002, Aug. 2020, doi: 10.1016/J.JCOMC.2020.100002.

[24] S. I. Thorsson, A. M. Waas, and M. Rassaian, "Low-velocity impact predictions of composite laminates using a continuum shell based modeling approach part A: Impact study," *Int J Solids Struct*, vol. 155, pp. 185–200, Dec. 2018, doi: 10.1016/J.IJSOLSTR.2018.07.020.

[25] J. Reiner, R. V.-P. of the A. S. for, and undefined 2018, "Progressive Axial Crushing of Composite Laminates: A Comparison Between LS-DYNA Continuum Damage Models," *researchgate.net*, doi: 10.12783/asc33/26071.

[26] D. E. Sommer, D. Thomson, J. Hoffmann, and N. Petrinic, "Numerical modelling of quasi-static and dynamic compact tension tests for obtaining the translaminar fracture toughness of CFRP," *Compos Sci Technol*, vol. 237, p. 109997, May 2023, doi: 10.1016/J.COMPSCITECH.2023.109997.

[27] X. Li, S. R. Hallett, M. R. Wisnom, N. Zobeiry, R. Vaziri, and A. Poursartip, "Experimental study of damage propagation in Over-height Compact Tension tests," *Compos Part A Appl Sci Manuf*, vol. 40, no. 12, pp. 1891–1899, Dec. 2009, doi: 10.1016/J.COMPOSITESA.2009.08.017.